THE METHOD OF FUNDAMENTAL SOLUTIONS FOR SOLVING DIRECT AND INVERSE SIGNORINI PROBLEMS IN ELASTICITY

ANDREAS KARAGEORGHIS AND DANIEL LESNIC

Abstract. The method of fundamental solutions (MFS) is a meshless boundary collocation method the implementation of which is very simple rendering the numerical solution of challenging boundary value problems such as free boundary and inverse problems. For this reason, in the current study we apply the MFS for the solution of a specific category of two–dimensional free boundary value problems in elasticity, namely, Signorini problems. We demonstrate that the proposed method is ideally suited for solving such problems. In the MFS, the displacement and traction are approximated by linear combinations of fundamental solutions with sources located outside the closure of the solution domain. The unknown coefficients in these expansions as well as the separation points on the Signorini boundary are determined by imposing/collocating the boundary conditions which can be of Dirichlet, Neumann or Signorini type. The MFS reformulation results in a constrained minimization problem which is solved using the MATLAB® optimization toolbox routine `fmincon`. The proposed technique is applied to problems from the literature previously solved using the boundary element method.

1. Introduction

Signorini problems in solid mechanics describe the deformation of an elastic body in contact with a rigid foundation [25, 37]. As such, these are contact problems in which on the known or unknown contact boundary, Dirichlet and Neumann conditions alternate in conjunction with certain inequality constraints [6, 13]. The problem is further complicated by the fact that the number and the location of the points where the change in the boundary conditions occurs are unknown [36]. Typical applications occur in beach percolation [1], electropainting [2], free surface problems [16], etc.

Since Signorini problems are contact boundary problems, the interest lies primarily on the boundary of the domain of the problem under consideration. For this reason, it is natural to apply boundary methods such as the boundary element method (BEM) for their solution, as evidenced by numerous applications to Signorini boundary value problems for the Laplace equation, see e.g., [3, 10, 18, 34, 36, 39, 42, 43]. On the other hand, the method of fundamental solutions (MFS) is a meshfree boundary method which, due to its simplicity, is suitable for the solution of problems in complex geometries, as demonstrated in the recent book [11]. Prior to this study, it has been applied to solve free boundary problems [19, 33, 35], see also [9], and direct Signorini potential problems in both two and three dimensions [31, 32, 44], using the `FORTRAN` NAG routine `E04UPF` [29]. More recently, two–dimensional direct and inverse Signorini problems for the Laplace equation were solved using

Date: March 28, 2025.
2000 *Mathematics Subject Classification.* Primary 65N35; Secondary 65N21, 65N38.
Key words and phrases. Signorini problem, method of fundamental solutions, elasticity.

the MFS in [22]. Note that the MFS has, in the last two decades, been employed extensively for the solution of various types of inverse problems [20, 21]. Moreover, Signorini problems in elasticity were considered, primarily using the BEM, in [14, 15, 17, 28, 30, 37, 38, 40, 41]. A related meshless method known as the backward substitution method has recently been used for the solution of three–dimensional linear elasticity boundary value problems [27]. To the best of our knowledge, this is the first time the MFS is applied to Signorini (including inverse) problems in elasticity.

The paper is structured as follows. In Section 2 we present the elasticity Signorini boundary value problems to be studied while in Section 3 we describe how the MFS is applied to such problems and provide extensive implementational details. The method is then applied to two numerical examples from the literature in Section 4. In Section 5 we show that the proposed method may be naturally adapted to solve inverse Signorini problems. Finally, in Section 6 we provide some conclusions and ideas for future work.

2. Signorini problems

We consider the two-dimensional Cauchy–Navier system in linear elasticity in the absence of body forces given by

$$\begin{cases} \mathcal{L}_1(u_1,u_2) \equiv \mu\,\Delta u_1 + \dfrac{\mu}{1-2\nu}\left(\dfrac{\partial^2 u_1}{\partial x^2} + \dfrac{\partial^2 u_2}{\partial x \partial y}\right) = 0, \\ \\ \mathcal{L}_2(u_1,u_2) \equiv \dfrac{\mu}{1-2\nu}\left(\dfrac{\partial^2 u_1}{\partial x \partial y} + \dfrac{\partial^2 u_2}{\partial y^2}\right) + \mu\,\Delta u_2 = 0, \end{cases} \quad \text{in } \Omega, \tag{2.1a}$$

for the displacement vector $\boldsymbol{u} = (u_1, u_2)$ subject to the Dirichlet boundary condition

$$\boldsymbol{u} = \boldsymbol{f}_1 \quad \text{on } \Gamma_1, \tag{2.1b}$$

the Neumann traction $\boldsymbol{t} = (t_1, t_2)$ boundary condition

$$\boldsymbol{t} = \boldsymbol{f}_2 \quad \text{on } \Gamma_2, \tag{2.1c}$$

and the contact conditions on the Signorini boundary

$$\mathbf{n}\cdot\boldsymbol{u} \le g, \quad \mathbf{n}\cdot\boldsymbol{t} \le 0, \quad \boldsymbol{\tau}\cdot\boldsymbol{t} = 0 \quad \text{on } \Gamma_{\rm s}, \tag{2.1d}$$

and

$$(\mathbf{n}\cdot\boldsymbol{t})\,(\mathbf{n}\cdot\boldsymbol{u} - g) = 0 \quad \text{on } \Gamma_{\rm s}, \tag{2.1e}$$

where $\mathbf{n} = (\mathrm{n}_x, \mathrm{n}_y)$ is the outward normal unit vector to the boundary, $\boldsymbol{\tau} = (\tau_x, \tau_y)$ is the tangential unit vector to the boundary, $\partial\Omega = \Gamma_1 \cup \Gamma_2 \cup \Gamma_{\rm s}$, $\Gamma_1 \cap \Gamma_2 = \Gamma_1 \cap \Gamma_{\rm s} = \Gamma_2 \cap \Gamma_{\rm s} = \emptyset$, $\boldsymbol{f}_1 = (f_{1_1}, f_{2_1})$ is given Dirichlet data on Γ_1, $\boldsymbol{f}_2 = (f_{1_2}, f_{2_2})$ is given Neumann data on Γ_2 and g is a given function describing the initial gap between the domain Ω of the elastic body and the rigid foundation. In (2.1a), the constant $\nu \in [0, 1/2)$ is Poisson's ratio and $\mu = E/\left(2(1+\nu)\right)$ is the shear modulus, where E is Young's modulus. The traction vector, $\boldsymbol{t} = (t_1, t_2)$ in (2.1c) and (2.1d) is given by

$$t_1 = 2\mu\left[\left(\frac{1-\nu}{1-2\nu}\right)\frac{\partial u_1}{\partial x} + \left(\frac{\nu}{1-2\nu}\right)\frac{\partial u_2}{\partial y}\right]\mathrm{n}_x + \mu\left[\frac{\partial u_1}{\partial y} + \frac{\partial u_2}{\partial x}\right]\mathrm{n}_y,$$

$$t_2 = \mu \left[\frac{\partial u_1}{\partial y} + \frac{\partial u_2}{\partial x} \right] \mathrm{n}_x + 2\mu \left[\left(\frac{\nu}{1-2\nu} \right) \frac{\partial u_1}{\partial x} + \left(\frac{1-\nu}{1-2\nu} \right) \frac{\partial u_2}{\partial y} \right] \mathrm{n}_y.$$

In (2.1d), the first constraint represent the non-penetration condition, the second constraint represents the direction of the surface pressure and the third constraint stands for the absence of friction [5] (in case of friction, see [15]). Also, (2.1e) represents the complementary condition, which states that at any point on the contact boundary not in contact with the foundation, the traction in the normal direction is zero [5]. The configuration of boundary value problem (2.1) is shown in Figure 1.

Using variational inequalities it can be established that the direct problem (2.1a)–(2.1e) has a unique weak solution, see e.g., [12] and [30, p.113].

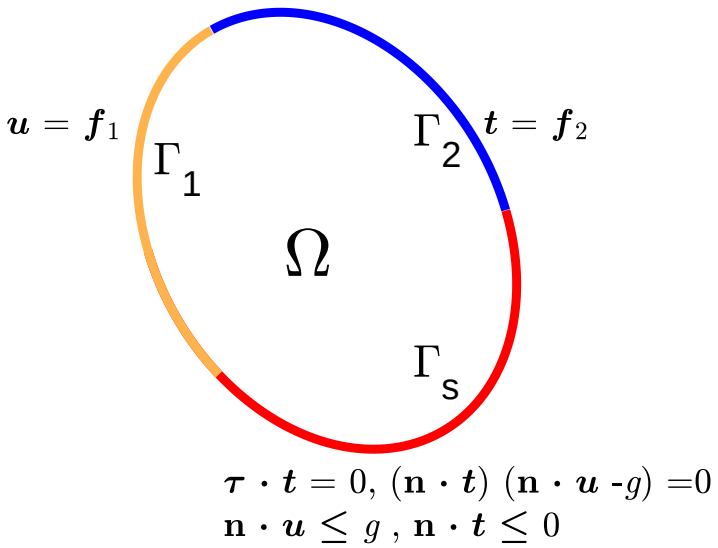

FIGURE 1. Geometry and boundary conditions of the Signorini problem (2.1).

3. THE METHOD OF FUNDAMENTAL SOLUTIONS (MFS)

We approximate the components of the displacement vector as

$$u_\ell(\boldsymbol{x}) \approx u_{\ell_N}(\boldsymbol{x}) = \sum_{n=1}^{N} U(\boldsymbol{x}, \boldsymbol{\xi}_n) d_{\ell_n}, \quad \boldsymbol{x} \in \overline{\Omega},\ \ell = 1, 2, \tag{3.1}$$

where $\boldsymbol{d}^\ell = (d_{\ell_n})_{n=1}^N$ for $\ell = 1, 2$ are $2N$ unknown coefficients and

$$U(\boldsymbol{x}, \boldsymbol{\xi}) = \frac{1}{8\,\pi\,\mu(1-\nu)} \left[-(3-4\,\nu)\,\log|\boldsymbol{x}-\boldsymbol{\xi}|\,I + \frac{(\boldsymbol{x}-\boldsymbol{\xi}) \otimes (\boldsymbol{x}-\boldsymbol{\xi})}{|\boldsymbol{x}-\boldsymbol{\xi}|^2} \right], \tag{3.2}$$

(with $\boldsymbol{x} = (x, y)$, $\boldsymbol{\xi} = (\xi_x, \xi_y)$) is the fundamental solution of the two–dimensional Lamé system of elasticity. Also, the points $(\boldsymbol{\xi}_n)_{n=1}^N \in \mathbb{R}^2 \backslash \overline{\Omega}$ are the 'singularities' (or sources) associated with the fundamental solution.

The components of the traction vector are approximated by

$$t_\ell(\boldsymbol{x}) \approx t_{\ell_N}(\boldsymbol{x}) = \sum_{n=1}^{N} T(\boldsymbol{x}, \boldsymbol{\xi}_n) d_{\ell_n}, \quad \boldsymbol{x} \in \overline{\Omega},\ \ell = 1, 2, \tag{3.3}$$

where T is the two–dimensional fundamental solution for the traction tensor in elasticity given by, see e.g. [4],

$$\begin{aligned} T_{1j}(\boldsymbol{x}, \boldsymbol{\xi}) = \frac{2\mu}{1-2\,\nu} \left[(1-\nu) \frac{\partial U_{1j}}{\partial x}(\boldsymbol{x}, \boldsymbol{\xi}) + \nu \frac{\partial U_{2j}}{\partial y}(\boldsymbol{x}, \boldsymbol{\xi}) \right] \mathrm{n}_x(\boldsymbol{x}) \\ + \mu \left[\frac{\partial U_{1j}}{\partial y}(\boldsymbol{x}, \boldsymbol{\xi}) + \frac{\partial U_{2j}}{\partial x}(\boldsymbol{x}, \boldsymbol{\xi}) \right] \mathrm{n}_y(\boldsymbol{x}), \quad j = 1, 2, \end{aligned}$$

$$\begin{aligned} T_{2j}(\boldsymbol{x}, \boldsymbol{\xi}) = \mu \left[\frac{\partial U_{1j}}{\partial y}(\boldsymbol{x}, \boldsymbol{\xi}) + \frac{\partial U_{2j}}{\partial x}(\boldsymbol{x}, \boldsymbol{\xi}) \right] \mathrm{n}_x(\boldsymbol{x}) \\ + \frac{2\mu}{1-2\,\nu} \left[\nu \frac{\partial U_{1j}}{\partial x}(\boldsymbol{x}, \boldsymbol{\xi}) + (1-\nu) \frac{\partial U_{2j}}{\partial y}(\boldsymbol{x}, \boldsymbol{\xi}) \right] \mathrm{n}_y(\boldsymbol{x}), \quad j = 1, 2. \end{aligned}$$

We place M_1 collocation points $(\boldsymbol{x}_m)_{m=1}^{M_1}$ on Γ_1, M_2 collocation points $(\boldsymbol{x}_m)_{m=M_1+1}^{M_1+M_2}$ on Γ_2 and M_s collocation points $(\boldsymbol{x}_m)_{m=M_1+M_2+1}^{M_1+M_2+M_\mathrm{s}}$ on Γ_s. We denote the total number of collocation points by $M = M_1 + M_2 + M_\mathrm{s}$. We also spread the N sources $(\boldsymbol{\xi}_n)_{n=1}^N$ on an enlarged pseudo–boundary similar to $\partial\Omega$. More specifically, we first distribute N points $\left(\widehat{\boldsymbol{\xi}}_k\right)_{n=1}^N$ as uniformly as possible on $\partial\Omega$. We then define the source points

$$\boldsymbol{\xi}_n = \mathbf{x}_\mathrm{c} + \eta \left(\widehat{\boldsymbol{\xi}}_n - \mathbf{x}_\mathrm{c} \right), \quad n = 1, \ldots, N, \tag{3.5}$$

where $\mathbf{x}_\mathrm{c} = (\mathrm{x_c}, \mathrm{y_c})$ is the geometric centre of Ω and $\eta > 1$ is a prescribed dilation parameter.

3.1. **Implementation details.** There are $2N$ unknowns coefficients $\boldsymbol{d}^1$ and $\boldsymbol{d}^2$ in (3.1) which can be determined by imposing the boundary conditions (2.1b)–(2.1e). This is achieved by using the MATLAB® optimization toolbox routine `fmincon` which finds the constrained minimum of a scalar nonlinear multivariate function. In the past, the routine `lsqnonlin` which minimizes a sum of squares has been extensively utilized with the MFS in the context of inverse geometric problems. The choice of `fmincon` was made because of its ability to include both linear and nonlinear constraints thus accommodating those resulting from the first two conditions in (2.1d), see [22]. In addition, the routine offers the option of providing the gradient of the objective function being minimized, which leads to substantial savings in CPU time.

In particular, the scalar function $F(\boldsymbol{d}^1,\boldsymbol{d}^2)$, which is to be minimized by the routine `fmincon`, is defined as follows. We denote

$$\begin{aligned}
\phi_m(\boldsymbol{d}^1,\boldsymbol{d}^2) &= u_{1_N}(\boldsymbol{x}_m)-f_{1_1}(\boldsymbol{x}_m), \quad m=1,\ldots,M_1,\\
\phi_{M_1+m}(\boldsymbol{d}^1,\boldsymbol{d}^2) &= u_{2_N}(\boldsymbol{x}_m)-f_{2_1}(\boldsymbol{x}_m), \quad m=1,\ldots,M_1,\\
\phi_{M_1+m}(\boldsymbol{d}^1,\boldsymbol{d}^2) &= t_{1_N}(\boldsymbol{x}_m)-f_{1_2}(\boldsymbol{x}_m), \quad m=M_1+1,\ldots,M_1+M_2,\\
\phi_{M_1+M_2+m}(\boldsymbol{d}^1,\boldsymbol{d}^2) &= t_{2_N}(\boldsymbol{x}_m)-f_{2_2}(\boldsymbol{x}_m), \quad m=M_1+1,\ldots,M_1+M_2,\\
\phi_{M_1+M_2+m}(\boldsymbol{d}^1,\boldsymbol{d}^2) &= t_{1_N}(\boldsymbol{x}_m)\tau_x(\boldsymbol{x}_m)+t_{2_N}(\boldsymbol{x}_m)\tau_y(\boldsymbol{x}_m),\\
&\quad m=M_1+M_2+1,\ldots,M_1+M_2+M_{\rm s},\\
\phi_{M_1+M_2+M_{\rm s}+m}(\boldsymbol{d}^1,\boldsymbol{d}^2) &= \Big(t_{1_N}(\boldsymbol{x}_m){\rm n}_x(\boldsymbol{x}_m)+t_{2_N}(\boldsymbol{x}_m){\rm n}_y(\boldsymbol{x}_m)\Big)\\
&\times \Big(u_{1_N}(\boldsymbol{x}_m){\rm n}_x(\boldsymbol{x}_m)+u_{2_N}(\boldsymbol{x}_m){\rm n}_y(\boldsymbol{x}_m)-g(\boldsymbol{x}_m)\Big)\\
&\quad m=M_1+M_2+1,\ldots,M_1+M_2+M_{\rm s},
\end{aligned} \tag{3.6}$$

where $\boldsymbol{\phi}(\boldsymbol{d}^1,\boldsymbol{d}^2)=\big(\phi_1(\boldsymbol{d}^1,\boldsymbol{d}^2),\phi_2(\boldsymbol{d}^1,\boldsymbol{d}^2),\ldots,\phi_{2M}(\boldsymbol{d}^1,\boldsymbol{d}^2)\big)$, and define

$$F(\boldsymbol{d}^1,\boldsymbol{d}^2)=||\boldsymbol{\phi}(\boldsymbol{d}^1,\boldsymbol{d}^2)||_2^2=\sum_{m=1}^{2M}\phi_m^2(\boldsymbol{d}^1,\boldsymbol{d}^2). \tag{3.7}$$

Moreover, we have the $2M_{\rm s}$ linear constraints

$$\mathbf{n}(\boldsymbol{x}_m)\cdot\boldsymbol{u}_N(\boldsymbol{x}_m)\le g(\boldsymbol{x}_m) \quad\text{and}\quad \mathbf{n}(\boldsymbol{x}_m)\cdot\boldsymbol{t}_N(\boldsymbol{x}_m)\le 0, \quad m=M_1+M_2+1,\ldots,M_1+M_2+M_{\rm s}, \tag{3.8}$$

which may be recast in the form

$$A\begin{pmatrix}\boldsymbol{d}^1\\ \boldsymbol{d}^2\end{pmatrix}\le\boldsymbol{b}, \tag{3.9}$$

where A is a $2M_{\rm s}\times 2N$ matrix and $\boldsymbol{b}$ is a $2M_{\rm s}\times 1$ vector. We also provide the gradient of the function F in (3.7) given by

$$\nabla F(\boldsymbol{d}^1,\boldsymbol{d}^2)=\boldsymbol{\Psi}(\boldsymbol{d}^1,\boldsymbol{d}^2)=\begin{bmatrix}\dfrac{\partial F(\boldsymbol{d}^1,\boldsymbol{d}^2)}{\partial\boldsymbol{d}^1}\\[2ex] \dfrac{\partial F(\boldsymbol{d}^1,\boldsymbol{d}^2)}{\partial\boldsymbol{d}^2}\end{bmatrix}, \tag{3.10}$$

where

$$\frac{\partial F(\boldsymbol{d}^1,\boldsymbol{d}^2)}{\partial\boldsymbol{d}^\ell}=\left(\frac{\partial F(\boldsymbol{d}^1,\boldsymbol{d}^2)}{\partial d_{\ell_n}}\right)_{n=1}^{N}, \quad \ell=1,2.$$

Clearly, $\boldsymbol{\Psi}(\boldsymbol{d}^1,\boldsymbol{d}^2)$ is a $2N\times 1$ vector with $\boldsymbol{\Psi}(\boldsymbol{d}^1,\boldsymbol{d}^2)=\big[\Psi_1(\boldsymbol{d}^1,\boldsymbol{d}^2),\Psi_2(\boldsymbol{d}^1,\boldsymbol{d}^2),\ldots,\Psi_{2N}(\boldsymbol{d}^1,\boldsymbol{d}^2)\big]^{\rm T}$. The minimization process terminates when either a user–specified tolerance `tol` is met (after a number of iterations `niter`) or a user–specified maximum number of iterations `maxiter` is reached. Note that `fmincon` also accommodates nonlinear constraints of the form

$$\boldsymbol{c}(\boldsymbol{d}^1,\boldsymbol{d}^2)\le\mathbf{0}. \tag{3.11}$$

Finally, we should mention that the user may provide `fmincon` with the vectors **lb** and **ub** which are the lower and upper bound vectors for the vector of unknowns **x**, which in this case is

$$\mathbf{x} = \begin{pmatrix} \boldsymbol{d}^1 \\ \boldsymbol{d}^2 \end{pmatrix} \quad \text{and we have} \quad \mathbf{lb} \leq \mathbf{x} \leq \mathbf{ub}.$$

4. Numerical examples

In all examples we took the initial guess to be

$$\mathbf{x}^{(0)} = \begin{pmatrix} \boldsymbol{d}^{1^{(0)}} \\ \boldsymbol{d}^{2^{(0)}} \end{pmatrix} = \begin{pmatrix} \mathbf{0} \\ \mathbf{0} \end{pmatrix}$$

and set `tol`$=10^{-14}$ and `maxiter` $\in [2000, 10000]$. All numerical computations for the results reported in this paper were carried out using MATLAB® R2024a on an x64-based processor, Intel(R) Core(TM) i5-10310U CPU @ 1.70GHz, 32 GB memory. The input data for the examples were taken from [14, 37, 40].

4.1. **Example 1.** We consider an elastic deformable square body $\Omega = (0, 10) \times (0, 10)$ in contact with a rigid foundation and gap $g = 0$. We take $\Gamma_{\rm s} = (0, 10) \times \{0\}$ and prescribe Neumann boundary conditions as $\boldsymbol{t} = \boldsymbol{f}_2 = (0, -1)$ on $(5, 10) \times \{10\}$, $\boldsymbol{t} = \boldsymbol{f}_2 = (1, 0)$ on $\{0\} \times (5, 10)$ and $\boldsymbol{t} = \boldsymbol{f}_2 = (0, 0)$ on $\{0\} \times (0, 5) \cup (0, 5) \times \{0\}$. Symmetry conditions are applied on $\{10\} \times (0, 10)$ as $\boldsymbol{u} \cdot \boldsymbol{n} = u_1 = 0$ and $\boldsymbol{t} \cdot \boldsymbol{\tau} = t_2 = 0$. The conditions on the Signorini boundary $\Gamma_{\rm s} = (0, 10) \times \{0\}$ are $-u_2 \leq 0$, $-t_2 \leq 0$, $t_1 = 0$ and $u_2 \cdot t_2 = 0$. The geometry and boundary conditions of this example are presented in Figure 2. As in [40], we took $E = 20000$ and $\nu = 0.3$.

We distributed 2M collocation points uniformly on the segments $\Gamma_{\rm s}$, and $\{10\} \times (0, 10)$, and M collocation points uniformly on the each of the segments $(0, 5) \times \{10\}$, $(5, 10) \times \{10\}$, $\{0\} \times (0, 5)$, and $\{0\} \times (5, 10)$ yielding a total of $M = 8$M collocation points. Note that here $M_{\rm s} = 2$M. The necessary details for the application of `fmincon` as well as the distribution of the collocation points in this example are provided in the Appendix.
In Figure 3 we present the results obtained for

(i) $M = N = 240$, `niter`$=2500$,
(ii) $M = N = 320$, `niter`$=3000$,
(iii) $M = N = 400$, `niter`$=2000$,

where in all cases $\eta = 1.023$. Note that the pseudo–boundary needs to be placed close to the physical boundary of the problem due to the boundary singularities at the points (5,10) and (0,5), see e.g. [26]. In particular, in Figures 3(a) and 3(b) we present the normal displacement $-u_2$ and the normal stress $-t_2$, respectively, on the Signorini boundary $\Gamma_{\rm s}$ for case (i). The initial and deformed configurations (magnified by 5000) of the body for the same case are presented in Figure 3(c). The corresponding results for increased numbers of $M = N$ given by the cases (ii) and (iii) are presented in Figures 3(d)–3(f) and Figures 3(g)–3(i), respectively. These results show the convergence of the numerical solution. Furthermore, they are in good agreement with the corresponding results presented in [14, 40].

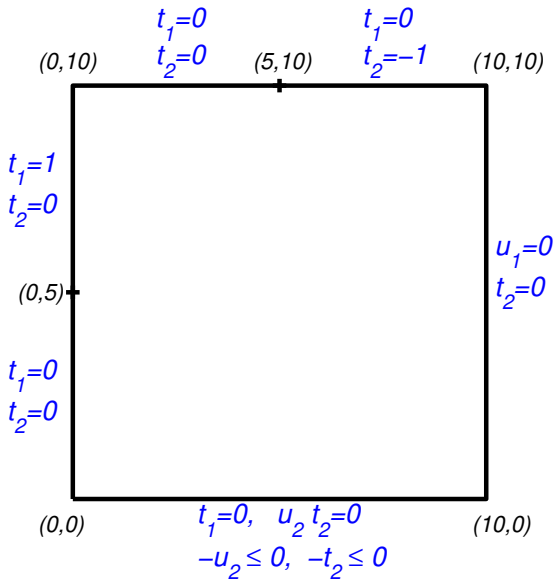

FIGURE 2. Example 1: Geometry and boundary conditions. The boundary values for the traction manifest discontinuities at the points $(5, 10)$ and $(10, 10)$ in t_2 and at the points $(0, 5)$ and $(0, 10)$ in t_1.

TABLE 1. Example 1: CPU times in seconds with number of iterations, with and without providing the gradient (3.10) for $M = N = 240$.

`niter`	With gradient	Without gradient
10	0.64	14.58
20	1.27	26.53
50	2.94	66.43
100	4.95	129.54
200	10.09	261.41
400	23.09	525.48

In Table 1 we present the CPU times required for different numbers of iterations when providing and when not providing the gradient (3.10) in case $M = N = 240$. Clearly, the savings when providing the gradient are considerable.

4.2. **Example 2.** We consider an elastic rectangular body $\Omega = (0, 3) \times (0, 1)$. In this case $\Gamma_s = (0, 3) \times \{0\}$. The Neumann boundary condition (2.1c) is given by $\boldsymbol{t} = \boldsymbol{f}_2 = (0, -2)$ on $\{3\} \times (0, 1)$ and $\boldsymbol{t} = \boldsymbol{f}_2 = (0, 0)$ on $(0, 3) \times \{1\}$. The Dirichlet boundary condition (2.1b) is

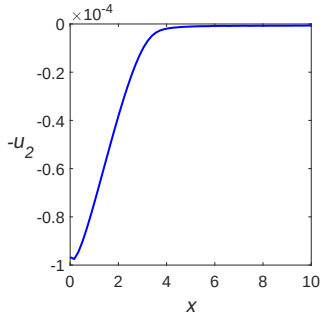

(a) -u_2 on Γ_s, $M = N = 240$

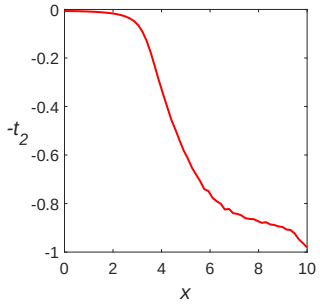

(b) -t_2 on Γ_s

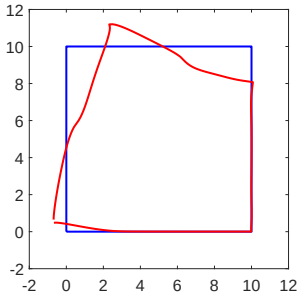

(c) Initial and deformed configurations

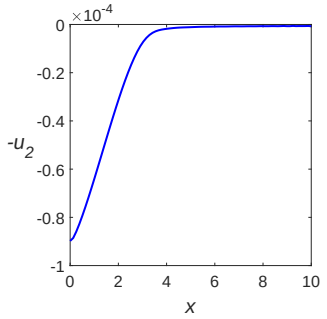

(d) -u_2 on Γ_s, $M = N = 320$

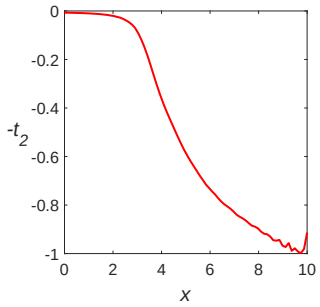

(e) -t_2 on Γ_s

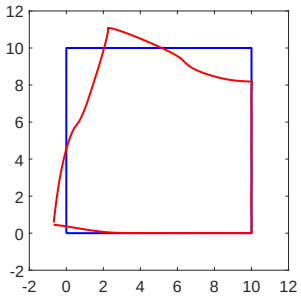

(f) Initial and deformed configurations

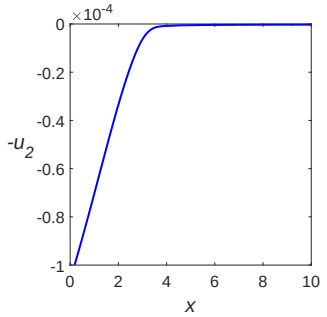

(g) -u_2 on Γ_s, $M = N = 400$

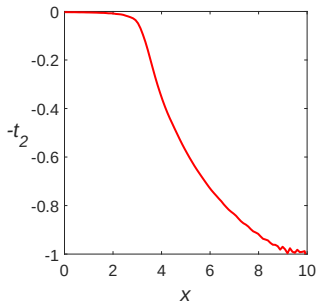

(h) -t_2 on Γ_s

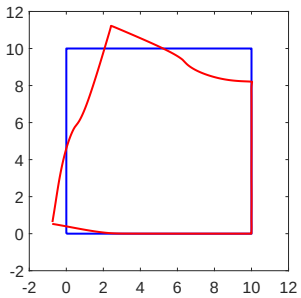

(i) Initial and deformed configurations

FIGURE 3. Example 1: Results for $M = N = 240$ ((a)–(c)), $M = N = 320$ ((d)–(f)), $M = N = 400$ ((g)–(i)).

$\boldsymbol{u} = \boldsymbol{f}_1 = (0,0)$ on $\Gamma_1 = \{0\} \times (0,1)$. We take the gap $g(x,y) = 0.003(x-1.5)^2 + 0.001$, which means that on the Signorini contact boundary $\Gamma_s = (0,3) \times \{0\}$ the boundary conditions (2.1d) and (2.1e) are:

$$-\left(u_2(x,0) + 0.003\,(x-1.5)^2 + 0.001\right) \le 0, \quad -t_2(x,0) \le 0, \quad t_1(x,0) = 0, \quad x \in (0,3),$$

and

$$t_2(x,0)\left(u_2(x,0)+0.003\,(x-1.5)^2+0.001\right)=0,\quad x\in(0,3).$$

The geometry and boundary conditions of Example 2 are presented in Figure 4. As in [40], we took $E=5000$ and $\nu=0.4$.

We distributed 3M collocation points uniformly on the segments $\Gamma_{\rm s}$ and $(0,3)\times\{1\}$, and M collocation points uniformly on the each of the segments $\{0\}\times(0,1)$ and $\{1\}\times(0,1)$, yielding a total of $M=8$M collocation points. Note that here $M_{\rm s}=3$M. The implementational details for the application of `fmincon` as well as the collocation points distribution in this example are provided in the Appendix.

In this example, because of the elongated shape of the domain Ω, in order to place the pseudo–boundary more uniformly close to the physical boundary of the problem, we modified (3.5) to

$$\xi_{x_n}=\mathrm{x_c}+\eta_x\left(\widehat{\xi}_{x_n}-\mathrm{x_c}\right),\quad \xi_{y_n}=\mathrm{y_c}+\eta_y\left(\widehat{\xi}_{y_n}-\mathrm{y_c}\right),\quad n=1,\ldots,N, \tag{4.1}$$

where $\eta_x=1+(\eta-1)/3$ and $\eta_y=\eta$. In Figure 5 we present the results obtained for:

(i) $M=N=240$, `niter`=3000,

(ii) $M=N=320$, `niter`=5000,

(iii) $M=N=400$, `niter`=9000,

where in all cases $\eta=1.17$. More specifically, in Figures 5(a) and 5(b) we present the normal displacement $-u_2$ and the normal traction $-t_2$, respectively, on the Signorini boundary $\Gamma_{\rm s}$ for case (i). The initial and deformed configurations (magnified by 20) of the body for the same case are presented in Figure 5(f). The corresponding results for increased numbers of $M=N$ given by the cases (ii) and (iii) are presented in Figures 5(d)–5(f) and Figures 5(g)–5(i), respectively. These results show the convergence of the numerical solution. Furthermore, they are consistent with the corresponding results presented in [37, 40].

5. Inverse Signorini problems

In reality, Signorini problems are actually inverse problems since the contact boundary $\Gamma_{\rm s}$ is, in general, unknown and has to be determined from some extra (non–intrusive) displacement measurements

$$\boldsymbol{u}=\boldsymbol{f}\quad\text{on }\Gamma, \tag{5.1}$$

on a non–zero measure sub–portion Γ of Γ_2. The inverse Signorini problem then requires determining the contact boundary $\Gamma_{\rm s}$ along with the displacement $\boldsymbol{u}$ satisfying equations (2.1a)–(2.1e) and (5.1). In case Ω is a connected domain, $\boldsymbol{f}_1=\boldsymbol{0}$, $g=0$, $\left(H^{-1/2}(\Gamma_2)\right)^2\ni\boldsymbol{f}_2\not\equiv 0$ and the endpoints of $\Gamma_{\rm s}$ are known, the solution $\boldsymbol{u}\in\left(H^1(\Omega)\right)^2$ and $\Gamma_{\rm s}\in C^{1,1}$ of this inverse problem is unique [7].

With reference to Example 2, we consider the solution domain Ω bounded by the segments $\{0\}\times(0,1)$, $(0,3)\times\{1\}$ and $\{3\}\times(0,1)$, and the contact boundary being represented by the graph of an unknown function $y\in C^{1,1}(0,3)$ with known ends $y(0)=y(3)=0$, namely,

$$\Gamma_{\rm s}=\{(x,y)|y=y(x),\,x\in(0,3)\}\,. \tag{5.2}$$

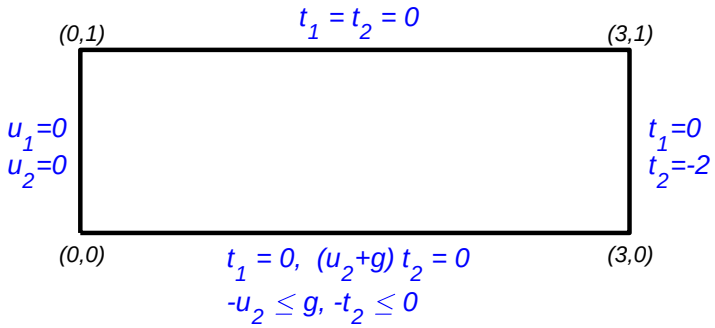

FIGURE 4. Example 2: Geometry and boundary conditions.

In the process of imposing the physical constraints (2.1d) and (2.1e) on this boundary we need to use that

$$\mathbf{n}(x,y(x))=\frac{1}{\sqrt{1+(y'(x))^2}}\,(y'(x),-1)\,,\ \boldsymbol{\tau}(x,y(x))=\frac{1}{\sqrt{1+(y'(x))^2}}\,(1,y'(x))\,,\ x\in(0,3). \tag{5.3}$$

The Dirichlet boundary condition (2.1b) is given by

$$\boldsymbol{u}=\boldsymbol{f}_1=\mathbf{0}\quad\text{on}\quad\Gamma_1=\{0\}\times(0,1), \tag{5.4}$$

and the Neumann boundary condition (2.1c) on $\Gamma_2=((0,3)\times\{1\})\cup(\{3\}\times(0,1))$ is given by

$$\boldsymbol{t}=\boldsymbol{f}_2=\begin{cases}(0,0) & \text{on } (0,3)\times\{1\},\\ (0,-2) & \text{on } \{3\}\times(0,1).\end{cases} \tag{5.5}$$

As in Example 2, we take $E=5000$, $\nu=0.4$ and $g(x,y(x))=0.003(x-1.5)^2+0.001$ for $x\in(0,3)$. We also assume that the displacement in (5.1) is measured on the top boundary $\Gamma=(0,3)\times\{1\}$.

In the inverse problem, since the contact boundary $\Gamma_{\rm s}$ is unknown, the functional which is minimized will also depend (through (5.2)) on y, and it will also incorporate the measurement (5.1).

We generated the Cauchy data (u_1,u_2) at 60 points on the top boundary by solving the direct boundary value problem in Example 2 with $M=N=240$ (M = N = 30), $\eta=1.17$ and `niter`=3000.

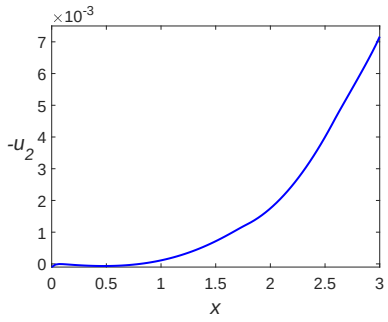

(a) -u_2 on Γ_s, $M = N = 240$

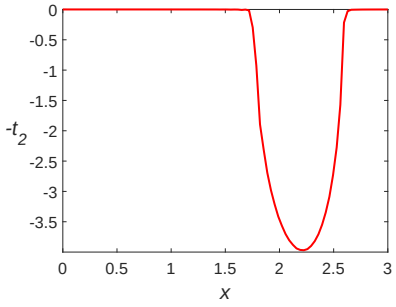

(b) -t_2 on Γ_s

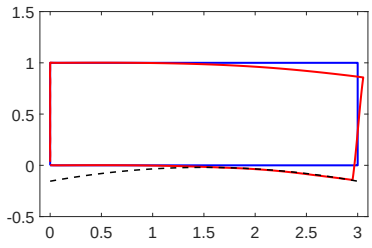

(c) Initial and deformed configurations

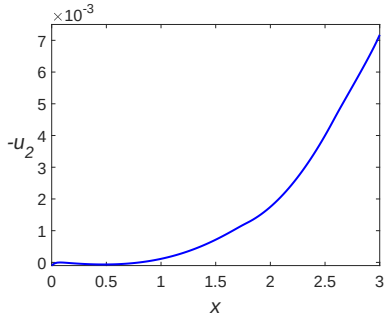

(d) -u_2 on Γ_s, $M = N = 320$

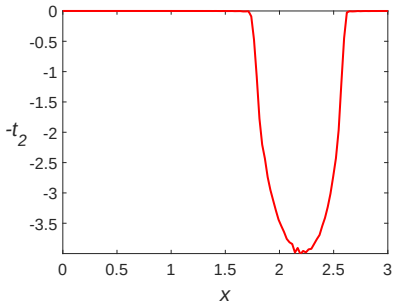

(e) -t_2 on Γ_s

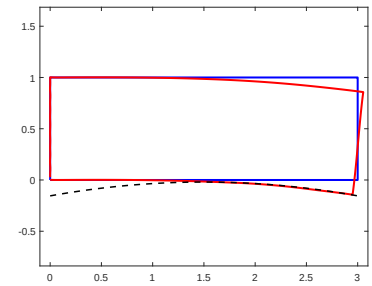

(f) Initial and deformed configurations

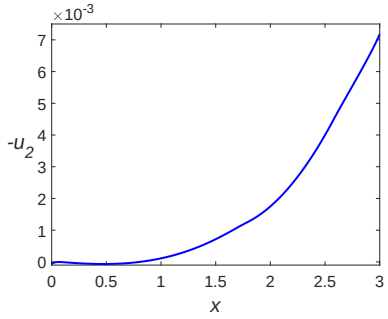

(g) -u_2 on Γ_s, $M = N = 400$

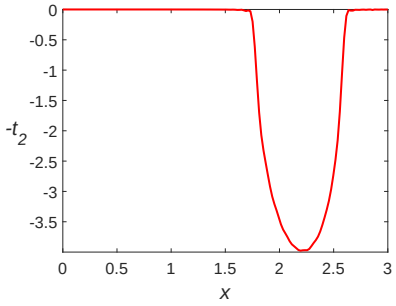

(h) -t_2 on Γ_s

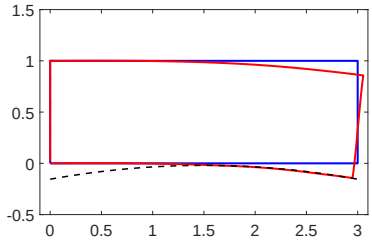

(i) Initial and deformed configurations

FIGURE 5. Example 2: Results for $M = N = 240$ ((a)–(c)), $M = N = 320$ ((d)–(f)), $M = N = 400$ ((g)–(i)).

We also added noise to the Cauchy data by taking

$$(\hat{u}_1(\boldsymbol{x}_j), \hat{u}_2(\boldsymbol{x}_j)) = (1 + \rho_j\, p)\, (u_1(\boldsymbol{x}_j), u_2(\boldsymbol{x}_j)), \quad j = \mathrm{M}+1, \ldots, 4\mathrm{M}, \tag{5.6}$$

where p represents the percentage of noise added to the Cauchy data on the top boundary $(0,3)\times\{1\}$ and ρ_j is a pseudo–random noisy variable drawn from a uniform distribution in $[-1,1]$ using the MATLAB® command `-1+2*rand(1,3M)`.

The initial guessed location of the boundary Γ_s was taken to be the parabola

$$y(x)=\frac{1}{10}x(3-x),\quad x\in[0,3].$$

In the inverse problem, to avoid an inverse crime, we took M = N = 20, meaning that we have $22\mathrm{M}=440$ collocation equations to satisfy in $16\mathrm{N}+3\mathrm{M}=380$ unknowns (the coefficients $\boldsymbol{d}^1,\boldsymbol{d}^2$ and the 3M heights $\mathbf{h}$ of the points on the Signorini boundary Γ_s). In this instance, the use of the lower and upper bound vectors for the unknowns is particularly useful, especially for the heights $\mathbf{h}$. Noting that now

$$\mathbf{x}=\begin{pmatrix}\boldsymbol{d}^1\\ \boldsymbol{d}^2\\ \mathbf{h}\end{pmatrix}$$

we took

$$\mathbf{lb}=\begin{pmatrix}-\mathbf{10}^{10}\\ -\mathbf{10}^{10}\\ -\mathbf{0.5}\end{pmatrix}\ \text{ and }\ \mathbf{ub}=\begin{pmatrix}\mathbf{10}^{10}\\ \mathbf{10}^{10}\\ \mathbf{0.5}\end{pmatrix}.$$

We also took $\eta=1.19$. Further details regarding the solution of the inverse problem are provided in the Appendix.

In Figures 6, 7, 8 and 9, we present the results for the reconstructed boundary Γ_s (in red dots) obtained using various numbers of iterations `niter` for noise p =0%, 3%, 6% and 9%, respectively. Note that for the higher amounts of p =6% and 9% noise, when `maxiter` is set to 2000, the maximum number of iterations before `tol` is reached is at lower values of 1136 and 438, respectively. These earlier stopping numbers of iterations also act as some form of regularization, which is necessary to be applied in order to restore stability of the inverse and ill–posed Signorini problem when the noise in the input Cauchy data (5.6) becomes significant. On comparison with the true boundary $\Gamma_s=\{(x,0)|x\in[0,3]\}$, the numerical results presented in Figures 6–9 show good accuracy and stability.

6. Discussion and conclusions

In this work, we considered the application of the MFS to two–dimensional Signorini boundary value contact problems in linear elasticity. The linear or nonlinear inequality constraints which appear in such problems have been incorporated in the minimization procedure in a natural way, when using the flexible and robust MATLAB® toolbox routine `fmincon`. In it, we have provided the gradient of the objective function (3.7) which leads to substantial savings in computational time. The MFS has been applied to two physical problems from the literature yielding results consistent with those previously obtained with the BEM. The analysis was further extended successfully to solving inverse Signorini problems in linear elasticity.

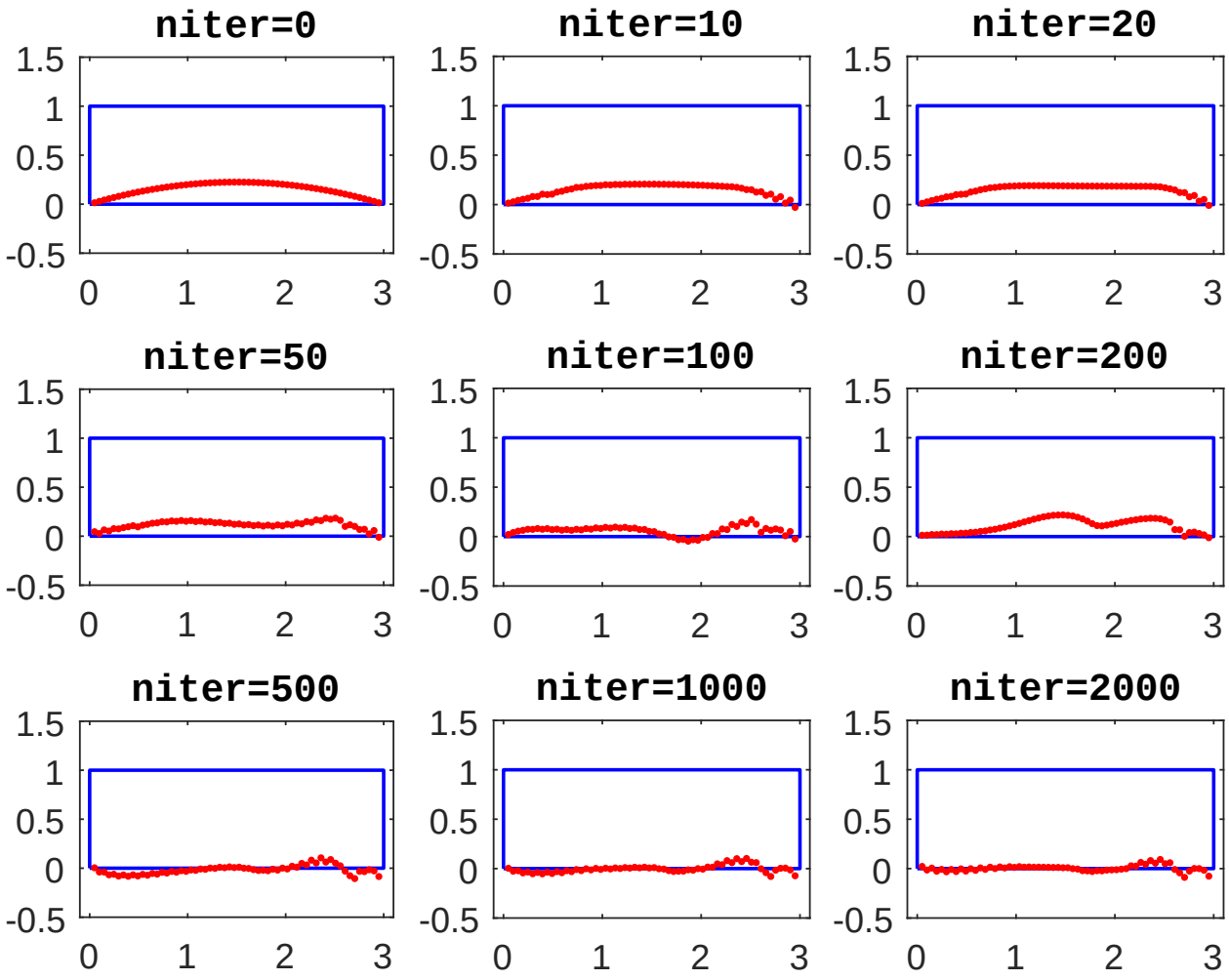

FIGURE 6. Inverse problem: Results with no noise for different numbers of iterations.

In the MFS, the fictitious boundary containing the source points entering the expansion (3.1) was placed at a fixed distance from the boundary $\partial\Omega$. For the first direct problem (Example 1 in Section 4.1), due to the presence of boundary singularities, the fictitious boundary was placed very close to the physical boundary $\partial\Omega$, as stated in the text and recommended in the literature [26]. For the second direct problem (Example 2 in Section 4.2), due to the elongated shape of the domain of the problem in question the fictitious boundary position was placed according to equation (4.1). In this case, the solution was less sensitive to the position of the pseudo–boundary than in Example 1.

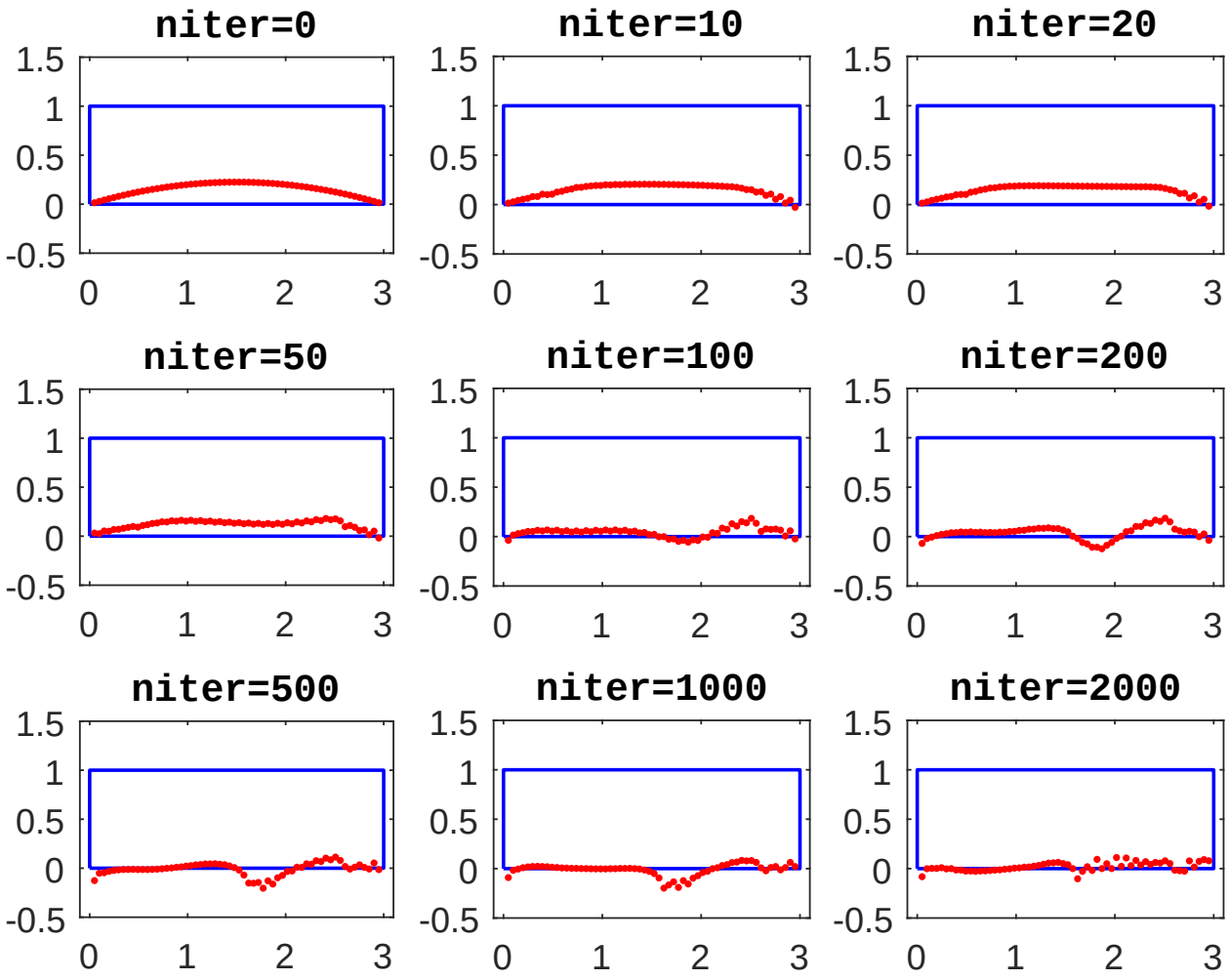

FIGURE 7. Inverse problem: Results with p =3% noise for different numbers of iterations.

In the inverse problem considered in Section 5, the position of the fictitious boundary was adjusted according to the moving boundary as explained in the Appendix (Inverse problem). Alternatively, one could use the leave–one–out cross validation (LOOCV) technique [8] to determine an appropriate location of the pseudo–boundary containing the source points in the MFS expansion (3.1). However, we have not used this approach in our work as it would render the overall technique too tedious and expensive. On the other hand, an adaptive approach for the optimal pseudo–boundary placement could be used, such as the one employed in [23], and this could be the subject of future research.

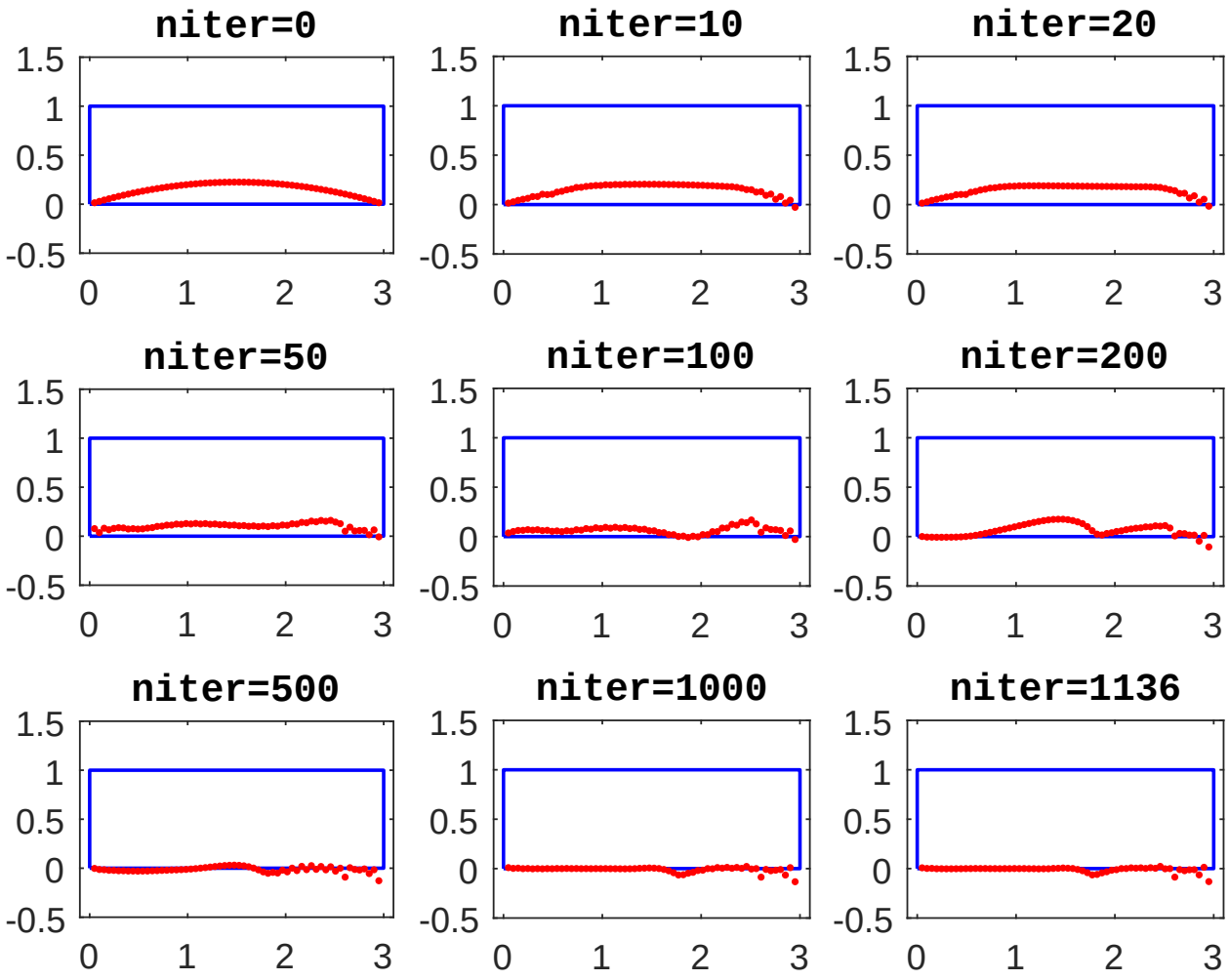

FIGURE 8. Inverse problem: Results with p =6% noise for different numbers of iterations.

As for the generality of the solution domain Ω, the fact that the domains in the direct problems (Examples 1 and 2) are rectangular is not a restriction or limitation, as the main difficulty lies rather with the complicated *alternating* boundary condition satisfaction which leads to a constrained minimization discrete problem. This is why the MFS is ideally suited for the numerical solution of such problems where the interest and difficulty are concentrated on the boundary. For the inverse problem examined, this difficulty is aggravated as now, as well as the determination of the separation point(s), one needs to determine the (unknown) position of part of the boundary. In future studies

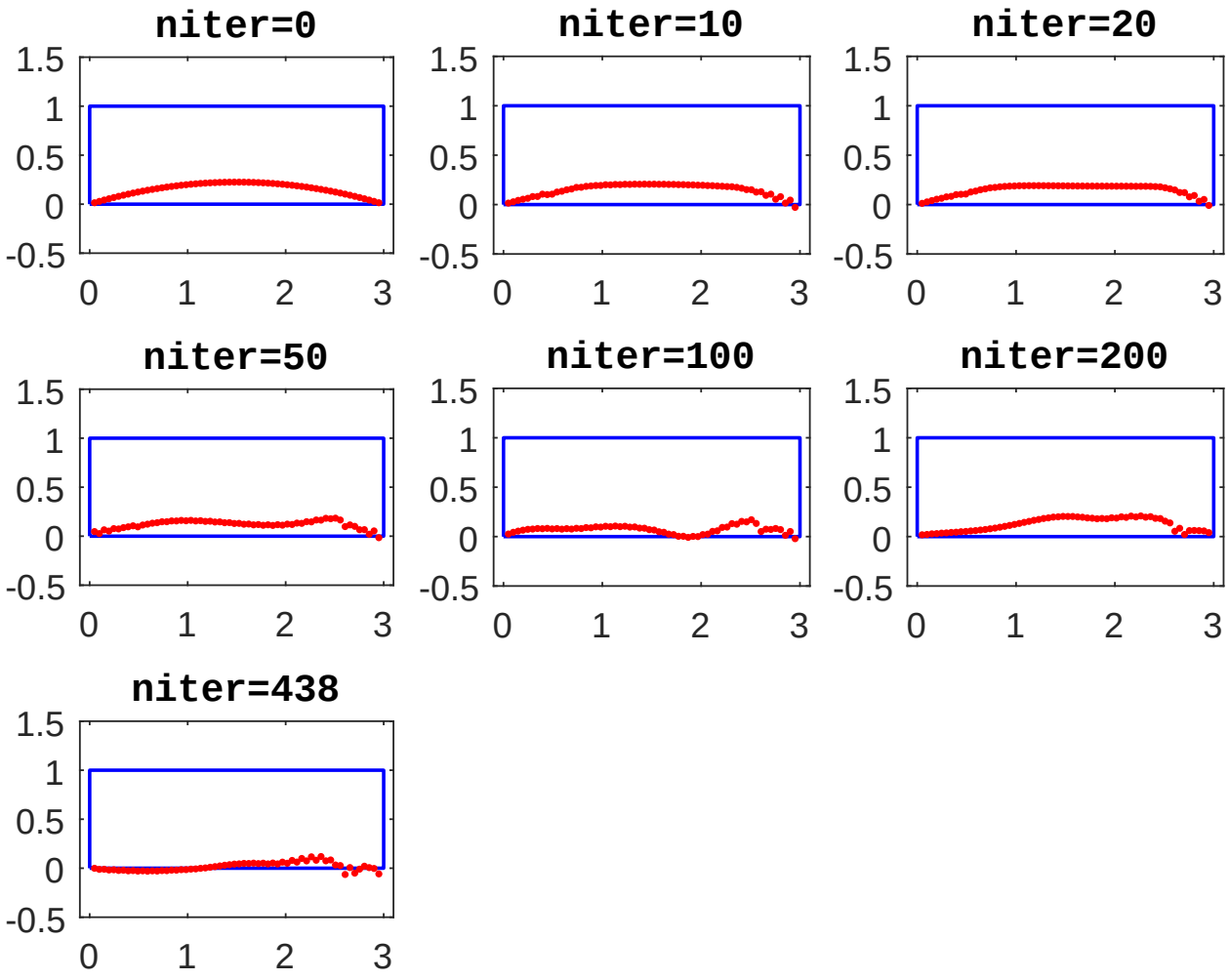

FIGURE 9. Inverse problem: Results with p =9% noise for different numbers of iterations.

we intend to work on elasticity Signorini problems in more irregular domains, as well as three–dimensional geometries.

Disclosure statement

The authors report there are no competing interests to declare.

References

[1] J. M. Aitchison, C. M. Elliott, and J. R. Ockendon, *Percolation in gently sloping beaches*, IMA Journal of Applied Mathematics, **30** (1983), 269–287.

[2] J. M. Aitchison, A. A. Lacey, and M. Shillor, *A model for an electropaint process*, IMA Journal of Applied Mathematics, **33** (1984), 17–31.

[3] J. M. Aitchison and M. W. Poole, *A numerical algorithm for the solution of Signorini problems*, Journal of Computational and Applied Mathematics, **94** (1998), 55–67.

[4] M. H. Aliabadi, *The Boundary Element Method. Applications in Solids and Structures*, Volume 2, John Wiley and Sons, London, 2002.

[5] F. S. Attia, Z. Cai and G. Starke, *First-order system least squares for the Signorini contact problem in linear elasticity*, SIAM Journal on Numerical Analysis, **47** (2009), 3027–3043.

[6] C. Baiocchi and A. Capelo, *Variational and Quasivariational Inequalities*, John Wiley & Sons, Inc., New York, 1984.

[7] A. Ben Abda, S. Chaabane, F. El Dabaghi and M. Jaoua, *On a nonlinear geometrical inverse problem of Signorini type: identifiability and stability*, Mathematical Methods in the Applied Sciences, **21** (1998), 1379–1398.

[8] C.S. Chen, A. Karageorghis and Y. Li, *On choosing the location of the sources in the MFS*, Numerical Algorithms, **72** (2016), 107–130.

[9] F. Chen, B. Zheng, J Lin and W. Chen, *Numerical solution of steady–state free boundary problems using the singular boundary method*, Advances in Applied Mathematics and Mechanics, **13** (2021), 163–175.

[10] Y. Cheng, Z. Nie, Z. Fan, S. Ding, K. Liu and M. Ding, *A mixed variational inequality method for solving Signorini problems*, Engineering Analysis with Boundary Elements, **147** (2023), 59–68.

[11] A. H-D. Cheng, C. S. Chen and A. Karageorghis, *An Introduction to the Method of Fundamental Solutions*, World Scientific, Singapore, 2025.

[12] F. Chouly and P. Hild, *On convergence of the penalty method for unilateral contact problems*, Applied Numerical Mathematics, **65** (2013), 27–40.

[13] C. M. Elliott and J. R. Ockendon, *Weak and Variational Methods for Moving Boundary Problems*, Research Notes in Mathematics, Vol. 59, Pitman (Advanced Publishing Program), Boston, Mass., 1982.

[14] B. Hild and P. Laborde, *Quadratic finite element methods for unilateral contact problems*, Applied Numerical Mathematics, **41** (2002), 401–421.

[15] B. Hild and V. Lleras, *Residual error estimators for Coulomb friction*, SIAM Journal on Numerical Analysis, **47** (2009), 3550–3583.

[16] S. D. Howison, J. D. Morgan, and J. R. Ockendon, *A class of codimension-two free boundary problems*, SIAM Review, **39** (1997), 221–253.

[17] Z. Huang and X. Cheng, *An accelerated method of Uzawa algorithm in contact problems*, Computers and Mathematics with Applications, **127** (2022), 97–104.

[18] A. Karageorghis, *Numerical solution of a shallow dam problem by a boundary element method*, Computer Methods in Applied Mechanics and Engineering, **61** (1987), 265–276.

[19] A. Karageorghis, *The method of fundamental solutions for the solution of steady-state free boundary problems*, Journal of Computational Physics, **98** (1992), 119–128.

[20] A. Karageorghis, D. Lesnic, and L. Marin, *The MFS for inverse geometric problems*, Inverse Problems and Computational Mechanics (L. Munteanu L. Marin and V. Chiroiu, eds.), vol. 1, Editura Academiei, Bucharest, 2011, pp. 191–216.

[21] A. Karageorghis, D. Lesnic, and L. Marin, *A survey of applications of the MFS to inverse problems*, Inverse Problems in Science and Engineering, **19** (2011), 309–336.

[22] A. Karageorghis, D. Lesnic, and L. Marin, *The method of fundamental solutions for the solution of direct and inverse Signorini problems*, Computers and Structures, **151** (2015), 11–19.

[23] A. Karageorghis, D. Lesnic and L. Marin, *An efficient moving pseudo-boundary MFS for void detection*, Engineering Analysis with Boundary Elements, **147** (2023), 90–111.

[24] N. Kikuchi and J. T. Oden, *Contact Problems in Elasticity: A Study of Variational Inequalities and Finite Element Methods*, SIAM, Philadelphia, 1988.
[25] R. Kornhuber and R. Krausse, *Adaptive multigrid methods for Signorini's problem in linear elasticity*, Computing and Visualisation in Science, **4** (2001), 9–20.
[26] M. Li, C. S. Chen and A. Karageorghis, *The MFS for the solution of harmonic boundary value problems with non–harmonic boundary conditions*, Computers and Mathematics with Applications, **66** (2013), 2400–2424.
[27] M. Ma, J. Xu, J. Lu and J. Lin, *The novel backward substitution method for the simulation of three–dimensional time–harmonic elastic wave problems*, Applied Mathematics Letters, **150** (2024), Article ID 108963 (6 pages).
[28] M. Maischak and E. P. Stephan, *Adaptive hp-versions of boundary element methods for elastic contact problems*, Computational Mechanics, **39** (2007), 597–607.
[29] NAG(UK) Ltd, Wilkinson House, Jordan Hill Road, Oxford, UK, *Numerical Algorithms Group Library Mark 21*, 2007.
[30] J. T. Oden and S. J. Kim, *Interior penalty methods for finite element approximations of the Signorini problem in elastostatics*, Computers and Mathematics with Applications, **8** (1982), 35–56.
[31] A. Poullikkas, A. Karageorghis, and G. Georgiou, *The method of fundamental solutions for Signorini problems*, IMA Journal of Numerical Analysis, **18** (1998), 273–285.
[32] A. Poullikkas, A. Karageorghis, and G. Georgiou, *The numerical solution of three dimensional Signorini problems with the method of fundamental solutions*, Engineering Analysis with Boundary Elements, **25** (2001), 221–227.
[33] A. Poullikkas, A. Karageorghis, G. Georgiou, and J. Ascough, *The method of fundamental solutions for Stokes flows with a free surface*, Numeral Methods for Partial Differential Equations, **14** (1998), 667–678.
[34] Y. Ren and X. Li, *A meshfree method for Signorini problems using boundary integral equations*, Mathematical Problems in Engineering, **2014** (2014), Article ID 490127 (12 pages).
[35] B. Šarler, *Solution of a two–dimensional bubble shape in potential flow by the method of fundamental solutions*, Engineering Analysis with Boundary Elements, **30** (2006), 227–235.
[36] W. Spann, *On the boundary element method for the Signorini problem of the Laplacian*, Numerische Mathematik **65** (1993), 337–356.
[37] G. Stadler, *Path-following and augmented Lagrangian methods for contact problems in linear elasticity*, Journal of Computational and Applied Mathematics **203** (2007), 533–547.
[38] J. Wu and S. Zhang, *Boundary element and augmented Lagrangian methods for contact problem with Coulomb friction*, Mathematical Problems in Engineering **2020** (2020), Article ID 7490736 (10 pages).
[39] S. Zhang, *A projection iterative algorithm for the Signorini problem using the boundary element method*, Engineering Analysis with Boundary Elements **50** (2015), 313–319.
[40] S. Zhang and X. Li, *Boundary augmented Lagrangian method for contact problems in linear elasticity*, Engineering Analysis with Boundary Elements **61** (2015), 127–133.
[41] S. Zhang, X. Li and R. Ran, *Self–adaptive projection and boundary element methods for contact problems with Tresca friction*, Communications in Nonlinear Science and Numerical Simulation **68** (2019), 72–85.
[42] S. Zhang and J. Zhu, *The boundary element-linear complementarity method for the Signorini problem*, Engineering Analysis with Boundary Elements **36** (2012), 112–117.
[43] S. Zhang and J. Zhu, *A projection iterative algorithm boundary element method for the Signorini problem*, Engineering Analysis with Boundary Elements **37** (2013), 176–181.
[44] H. Zheng and X. Li, *Application of the method of fundamental solutions to 2D and 3D Signorini problems*, Engineering Analysis with Boundary Elements **58** (2015), 48–57.

Appendix

Example 1. The collocation points were distributed as follows (moving clockwise from the origin):

$$\boldsymbol{x}_m = \left(0, \frac{5m}{\mathrm{M}+1}\right), \quad \boldsymbol{x}_{\mathrm{M}+m} = \left(0, 5+\frac{5m}{\mathrm{M}+1}\right), \quad m = 1, \ldots, \mathrm{M},$$
$$\boldsymbol{x}_{2\mathrm{M}+m} = \left(\frac{5(m-1)}{\mathrm{M}}, 10\right), \quad \boldsymbol{x}_{3\mathrm{M}+m} = \left(5+\frac{5m}{\mathrm{M}}, 10\right), \quad m = 1, \ldots, \mathrm{M},$$
$$\boldsymbol{x}_{4\mathrm{M}+m} = \left(10, 10-\frac{10m}{2\mathrm{M}+1}\right), \quad \boldsymbol{x}_{6\mathrm{M}+m} = \left(10-\frac{10(m-1)}{2\mathrm{M}-1}, 0\right), \quad m = 1, \ldots, 2\mathrm{M}.$$

With reference to Section 3.1, we took for (3.7) (moving clockwise from the origin):

$$\phi_m(\boldsymbol{d}^1, \boldsymbol{d}^2) = t_{1_N}(\boldsymbol{x}_m), \quad \phi_{\mathrm{M}+m}(\boldsymbol{d}^1, \boldsymbol{d}^2) = t_{2_N}(\boldsymbol{x}_m), \quad m = 1, \ldots, \mathrm{M},$$
$$\phi_{\mathrm{M}+m}(\boldsymbol{d}^1, \boldsymbol{d}^2) = t_{1_N}(\boldsymbol{x}_m) - 1, \quad \phi_{2\mathrm{M}+m}(\boldsymbol{d}^1, \boldsymbol{d}^2) = t_{2_N}(\boldsymbol{x}_m), \quad m = \mathrm{M}+1, \ldots, 2\mathrm{M},$$
$$\phi_{2\mathrm{M}+m}(\boldsymbol{d}^1, \boldsymbol{d}^2) = t_{1_N}(\boldsymbol{x}_m), \quad \phi_{3\mathrm{M}+m}(\boldsymbol{d}^1, \boldsymbol{d}^2) = t_{2_N}(\boldsymbol{x}_m), \quad m = 2\mathrm{M}+1, \ldots, 3\mathrm{M},$$
$$\phi_{3\mathrm{M}+m}(\boldsymbol{d}^1, \boldsymbol{d}^2) = t_{1_N}(\boldsymbol{x}_m), \quad \phi_{4\mathrm{M}+m}(\boldsymbol{d}^1, \boldsymbol{d}^2) = t_{2_N}(\boldsymbol{x}_m) + 1, \quad m = 3\mathrm{M}+1, \ldots, 4\mathrm{M},$$
$$\phi_{4\mathrm{M}+m}(\boldsymbol{d}^1, \boldsymbol{d}^2) = u_{1_N}(\boldsymbol{x}_m), \quad \phi_{6\mathrm{M}+m}(\boldsymbol{d}^1, \boldsymbol{d}^2) = t_{2_N}(\boldsymbol{x}_m), \quad m = 4\mathrm{M}+1, \ldots, 6\mathrm{M},$$
$$\phi_{6\mathrm{M}+m}(\boldsymbol{d}^1, \boldsymbol{d}^2) = t_{1_N}(\boldsymbol{x}_m), \quad \phi_{8\mathrm{M}+m}(\boldsymbol{d}^1, \boldsymbol{d}^2) = u_{2_N}(\boldsymbol{x}_m) t_{2_N}(\boldsymbol{x}_m), \quad m = 6\mathrm{M}+1, \ldots, 8\mathrm{M},$$

and for the gradient (3.10),

$$\begin{aligned}
\Psi_{n+(\ell-1)N}(\boldsymbol{d}^1, \boldsymbol{d}^2) \;=\; & 2 \sum_{m=1}^{\mathrm{M}} \left[t_{1_N}(\boldsymbol{x}_m)\, T_{1\ell}(\boldsymbol{x}_m, \boldsymbol{\xi}_n) + t_{2_N}(\boldsymbol{x}_m)\, T_{2\ell}(\boldsymbol{x}_m, \boldsymbol{\xi}_n) \right] \\
+ \; & 2 \sum_{m=\mathrm{M}+1}^{2\mathrm{M}} \left[(t_{1_N}(\boldsymbol{x}_m) - 1)\; T_{1\ell}(\boldsymbol{x}_m, \boldsymbol{\xi}_n) + t_{2_N}(\boldsymbol{x}_m)\, T_{2\ell}(\boldsymbol{x}_m, \boldsymbol{\xi}_n) \right] \\
+ \; & 2 \sum_{m=2\mathrm{M}+1}^{3\mathrm{M}} \left[t_{1_N}(\boldsymbol{x}_m)\, T_{1\ell}(\boldsymbol{x}_m, \boldsymbol{\xi}_n) + t_{2_N}(\boldsymbol{x}_m) T_{2\ell}(\boldsymbol{x}_m, \boldsymbol{\xi}_n) \right] \\
+ \; & 2 \sum_{m=3\mathrm{M}+1}^{4\mathrm{M}} \left[t_{1_N}(\boldsymbol{x}_m)\, T_{1\ell}(\boldsymbol{x}_m, \boldsymbol{\xi}_n) + (t_{2_N}(\boldsymbol{x}_m) + 1)\; T_{2\ell}(\boldsymbol{x}_m, \boldsymbol{\xi}_n) \right] \\
+ \; & 2 \sum_{m=4\mathrm{M}+1}^{6\mathrm{M}} \left[u_{1_N}(\boldsymbol{x}_m)\, U_{1\ell}(\boldsymbol{x}_m, \boldsymbol{\xi}_n) + t_{2_N}(\boldsymbol{x}_m)\, T_{2\ell}(\boldsymbol{x}_m, \boldsymbol{\xi}_n) \right] \\
+ \; & 2 \sum_{m=6\mathrm{M}+1}^{8\mathrm{M}} \left[t_{1_N}(\boldsymbol{x}_m)\, T_{1\ell}(\boldsymbol{x}_m, \boldsymbol{\xi}_n) \right. \\
+ \; & \left. u_{2_N}(\boldsymbol{x}_m)\, U_{2\ell}(\boldsymbol{x}_m, \boldsymbol{\xi}_n) \cdot \left(t_{2_N}(\boldsymbol{x}_m)\right)^2 + t_{2_N}(\boldsymbol{x}_m)\, T_{2\ell}(\boldsymbol{x}_m, \boldsymbol{\xi}_n) \cdot \left(u_{2_N}(\boldsymbol{x}_m)\right)^2 \right],
\end{aligned}$$

for $\ell = 1, 2$ and $n = 1, \ldots, N$. Moreover, the linear constraints (3.8) become

$$-u_{2_N}(\boldsymbol{x}_m) \le 0 \quad \text{and} \quad -t_{2_N}(\boldsymbol{x}_m) \le 0, \quad m = 6\mathrm{M}+1, \ldots, 8\mathrm{M}.$$

Example 2. The collocation points were distributed as follows (moving clockwise from the origin):

$$\boldsymbol{x}_m = \left(0, \frac{m}{\mathrm{M}+1}\right), \quad \boldsymbol{x}_{4\mathrm{M}+m} = \left(3, 1 - \frac{m}{\mathrm{M}+1}\right), \quad m = 1, \ldots, \mathrm{M},$$
$$\boldsymbol{x}_{\mathrm{M}+m} = \left(0, \frac{3(m-1)}{3\mathrm{M}-1}\right), \quad \boldsymbol{x}_{5\mathrm{M}+m} = \left(3 - \frac{3(m-1)}{3\mathrm{M}-1}, 0\right), \quad m = 1, \ldots, 3\mathrm{M}.$$

With reference to Section 3.1, we took for (3.7) (moving clockwise from the origin):

$$\phi_m(\boldsymbol{d}^1, \boldsymbol{d}^2) = u_{1_N}(\boldsymbol{x}_m), \quad \phi_{\mathrm{M}+m}(\boldsymbol{d}^1, \boldsymbol{d}^2) = u_{2_N}(\boldsymbol{x}_m), \quad m = 1, \ldots, \mathrm{M},$$
$$\phi_{\mathrm{M}+m}(\boldsymbol{d}^1, \boldsymbol{d}^2) = t_{1_N}(\boldsymbol{x}_m), \quad \phi_{4\mathrm{M}+m}(\boldsymbol{d}^1, \boldsymbol{d}^2) = t_{2_N}(\boldsymbol{x}_m), \quad m = \mathrm{M}+1, \ldots, 4\mathrm{M},$$
$$\phi_{4\mathrm{M}+m}(\boldsymbol{d}^1, \boldsymbol{d}^2) = t_{1_N}(\boldsymbol{x}_m), \quad \phi_{5\mathrm{M}+m}(\boldsymbol{d}^1, \boldsymbol{d}^2) = t_{2_N}(\boldsymbol{x}_m) + 2, \quad m = 4\mathrm{M}+1, \ldots, 5\mathrm{M},$$
$$\phi_{5\mathrm{M}+m}(\boldsymbol{d}^1, \boldsymbol{d}^2) = t_{1_N}(\boldsymbol{x}_m), \quad \phi_{8\mathrm{M}+m}(\boldsymbol{d}^1, \boldsymbol{d}^2) = \left(u_{2_N}(\boldsymbol{x}_m) + g(\boldsymbol{x}_m)\right) t_{2_N}(\boldsymbol{x}_m), \quad m = 5\mathrm{M}+1, \ldots, 8\mathrm{M},$$

and for the gradient (3.10),

$$\begin{aligned}
\Psi_{n+(\ell-1)N}(\boldsymbol{d}^1, \boldsymbol{d}^2) \;=\; & 2 \sum_{m=1}^{\mathrm{M}} \left[u_{1_N}(\boldsymbol{x}_m)\, U_{1\ell}(\boldsymbol{x}_m, \boldsymbol{\xi}_n) + u_{2_N}(\boldsymbol{x}_m)\, U_{2\ell}(\boldsymbol{x}_m, \boldsymbol{\xi}_n)\right] \\
+ \; & 2 \sum_{m=\mathrm{M}+1}^{4\mathrm{M}} \left[t_{1_N}(\boldsymbol{x}_m)\, T_{1\ell}(\boldsymbol{x}_m, \boldsymbol{\xi}_n) + t_{2_N}(\boldsymbol{x}_m)\, T_{2\ell}(\boldsymbol{x}_m, \boldsymbol{\xi}_n)\right] \\
+ \; & 2 \sum_{m=4\mathrm{M}+1}^{5\mathrm{M}} \left[t_{1_N}(\boldsymbol{x}_m)\, T_{1\ell}(\boldsymbol{x}_m, \boldsymbol{\xi}_n) + \left(t_{2_N}(\boldsymbol{x}_m) + 2\right)\, T_{2\ell}(\boldsymbol{x}_m, \boldsymbol{\xi}_n)\right] \\
+ \; & 2 \sum_{m=5\mathrm{M}+1}^{8\mathrm{M}} \Big[t_{1_N}(\boldsymbol{x}_m)\, T_{1\ell}(\boldsymbol{x}_m, \boldsymbol{\xi}_n) \\
+ \; & \left(u_{2_N}(\boldsymbol{x}_m) + g(\boldsymbol{x}_m)\right)\, U_{2\ell}(\boldsymbol{x}_m, \boldsymbol{\xi}_n) \cdot \left(t_{2_N}(\boldsymbol{x}_m)\right)^2 \\
+ \; & t_{2_N}(\boldsymbol{x}_m)\, T_{2\ell}(\boldsymbol{x}_m, \boldsymbol{\xi}_n) \cdot \left(u_{2_N}(\boldsymbol{x}_m) + g(\boldsymbol{x}_m)\right)^2\Big],
\end{aligned}$$

for $\ell = 1, 2$ and $n = 1, \ldots, N$. Moreover, the linear constraints (3.8) become

$$-u_{2_N}(\boldsymbol{x}_m) \le g(\boldsymbol{x}_m) \quad \text{and} \quad -t_{2_N}(\boldsymbol{x}_m) \le 0, \quad m = 5\mathrm{M}+1, \ldots, 8\mathrm{M}.$$

Inverse problem. The collocation points and sources were taken exactly as in Example 2 with the exception of the points on Γ_{s} which were taken as

$$\boldsymbol{x}_{5\mathrm{M}+m} = \left(3 - \frac{3m}{3\mathrm{M}+1}, \mathrm{h}_m\right), \quad m = 1, \ldots, 3\mathrm{M},$$

where, via (5.2), the heights $\mathrm{h}_m := y\left(3 - \dfrac{3m}{3\mathrm{M}+1}\right)$ for $m = 1, \ldots, 3\mathrm{M}$ are unknown and have to be determined as part of the solution. In addition, the sources $(\boldsymbol{\xi}_n)_{n=5\mathrm{N}+1}^{8\mathrm{N}}$ (note that in this problem we took $\mathrm{N} = \mathrm{M}$) were adjusted at each iteration, as follows:

$$\boldsymbol{\xi}_{5\mathrm{N}+m} = \left(3 - \frac{3m}{3\mathrm{M}+1}, \mathrm{h}_m - \frac{(\eta-1)}{2}\right), \quad m = 1, \ldots, 3\mathrm{M}.$$

With this adjustment, the sources are kept outside the domain. Importantly, at the points $\boldsymbol{x}_m$, $m = 5\mathrm{M}+1, \ldots, 8\mathrm{M}$, on the Signorini boundary we require $\boldsymbol{\tau}$ and $\mathbf{n}$, which can be evaluated from (5.3). In these, the derivative y' is approximated using the central difference formulas

$$y'(\boldsymbol{x}_m) \approx \frac{y(\boldsymbol{x}_{m-1}) - y(\boldsymbol{x}_{m+1})}{2h}, \quad m = 5\mathrm{M}+2, \ldots, 8\mathrm{M}-1,$$

$$y'(\boldsymbol{x}_{5\mathrm{M}+1}) \approx -\frac{y(\boldsymbol{x}_{5\mathrm{M}+2})}{2h}, \quad y'(\boldsymbol{x}_{8\mathrm{M}}) \approx \frac{y(\boldsymbol{x}_{8\mathrm{M}-1})}{2h},$$

where $h = 3/(3\mathrm{M}+1)$. With reference to Section 5, we took for the objective functional (3.7) (moving clockwise from the origin):

$$\begin{aligned}
\phi_m(\boldsymbol{d}^1, \boldsymbol{d}^2, \mathbf{h}) &= u_{1_N}(\boldsymbol{x}_m), \quad m = 1, \ldots, \mathrm{M}, \\
\phi_{\mathrm{M}+m}(\boldsymbol{d}^1, \boldsymbol{d}^2, \mathbf{h}) &= u_{2_N}(\boldsymbol{x}_m), \quad m = 1, \ldots, \mathrm{M}, \\
\phi_{\mathrm{M}+m}(\boldsymbol{d}^1, \boldsymbol{d}^2, \mathbf{h}) &= t_{1_N}(\boldsymbol{x}_m), \quad m = \mathrm{M}+1, \ldots, 4\mathrm{M}, \\
\phi_{4\mathrm{M}+m}(\boldsymbol{d}^1, \boldsymbol{d}^2, \mathbf{h}) &= t_{2_N}(\boldsymbol{x}_m), \quad m = \mathrm{M}+1, \ldots, 4\mathrm{M}, \\
\phi_{7\mathrm{M}+m}(\boldsymbol{d}^1, \boldsymbol{d}^2, \mathbf{h}) &= u_{1_N}(\boldsymbol{x}_m) - \widehat{u}_{1_N}(\boldsymbol{x}_m), \quad m = \mathrm{M}+1, \ldots, 4\mathrm{M}, \\
\phi_{10\mathrm{M}+m}(\boldsymbol{d}^1, \boldsymbol{d}^2, \mathbf{h}) &= u_{2_N}(\boldsymbol{x}_m) - \widehat{u}_{2_N}(\boldsymbol{x}_m), \quad m = \mathrm{M}+1, \ldots, 4\mathrm{M}, \\
\phi_{10\mathrm{M}+m}(\boldsymbol{d}^1, \boldsymbol{d}^2, \mathbf{h}) &= t_{1_N}(\boldsymbol{x}_m), \quad m = 4\mathrm{M}+1, \ldots, 5\mathrm{M}, \\
\phi_{11\mathrm{M}+m}(\boldsymbol{d}^1, \boldsymbol{d}^2, \mathbf{h}) &= t_{2_N}(\boldsymbol{x}_m) + 2, \quad m = 4\mathrm{M}+1, \ldots, 5\mathrm{M}, \\
\phi_{11\mathrm{M}+m}(\boldsymbol{d}^1, \boldsymbol{d}^2, \mathbf{h}) &= t_{1_N}(\boldsymbol{x}_m)\tau_x(\boldsymbol{x}_m) + t_{2_N}(\boldsymbol{x}_m)\tau_y(\boldsymbol{x}_m), \quad m = 5\mathrm{M}+1, \ldots, 8\mathrm{M}, \\
\phi_{14\mathrm{M}+m}(\boldsymbol{d}^1, \boldsymbol{d}^2, \mathbf{h}) &= \Big(t_{1_N}(\boldsymbol{x}_m)\mathrm{n}_x(\boldsymbol{x}_m) + t_{2_N}(\boldsymbol{x}_m)\mathrm{n}_y(\boldsymbol{x}_m)\Big) \\
&\quad \times \Big(u_{1_N}(\boldsymbol{x}_m)\mathrm{n}_x(\boldsymbol{x}_m) + u_{2_N}(\boldsymbol{x}_m)\mathrm{n}_y(\boldsymbol{x}_m) - g(\boldsymbol{x}_m)\Big), \quad m = 5\mathrm{M}+1, \ldots, 8\mathrm{M},
\end{aligned}$$

where $\mathbf{h} := (\mathrm{h}_\ell)_{\ell=1}^{3\mathrm{M}}$, and $\widehat{u}_{1_N}(\boldsymbol{x}_m)$ and $\widehat{u}_{2_N}(\boldsymbol{x}_m)$ for $m = \mathrm{M}+1, \ldots, 4\mathrm{M}$ are the Cauchy data generated by solving the direct problem in Example 2. For the inverse problem, the analytical calculation of the gradient of (3.7) becomes too complicated and therefore is not considered. We also have the following nonlinear constraints (3.11) in `fmincon`:

$$\begin{aligned}
t_{1_N}(\boldsymbol{x}_m)\tau_x(\boldsymbol{x}_m) + t_{2_N}(\boldsymbol{x}_m)\tau_y(\boldsymbol{x}_m) \le 0, \quad m = 5\mathrm{M}+1, \ldots, 8\mathrm{M}, \\
\Big(t_{1_N}(\boldsymbol{x}_m)\mathrm{n}_x(\boldsymbol{x}_m) + t_{2_N}(\boldsymbol{x}_m)\mathrm{n}_y(\boldsymbol{x}_m)\Big) \times \Big(u_{1_N}(\boldsymbol{x}_m)\mathrm{n}_x(\boldsymbol{x}_m) + u_{2_N}(\boldsymbol{x}_m)\mathrm{n}_y(\boldsymbol{x}_m) - g(\boldsymbol{x}_m)\Big) \le 0, \\
m = 5\mathrm{M}+1, \ldots, 8\mathrm{M}.
\end{aligned}$$

Department of Mathematics and Statistics, University of Cyprus/ Πανεπιστημιο Κυπρου,
P.O.Box 20537, 1678 Nicosia/Λευκωσια, Cyprus/Κυπρος
E-mail address: andreask@ucy.ac.cy

Department of Applied Mathematics, University of Leeds, Leeds LS2 9JT, UK
E-mail address: amt5ld@maths.leeds.ac.uk